doi:10.3788/gzxb20154412.1211002

波像差的梯度偏离值评价方法

宋淑梅

(中国科学院长春光学精密机械与物理研究所,长春 130033)

摘 要:针对成像光学系统的波像差检测,提出波像差梯度偏离值评价方法,用于表征波前的成像性能.定义波像差梯度偏离值为波前成像点与成像能量中心的偏离值,相对波像差梯度偏离值为波像差梯度偏离值与艾里斑大小的比值.相对波像差梯度偏离值与波前口径、形状、焦距均无关,其与波像差梯度偏离值均可以用成像尺寸、成像集中度以及成像能量分布等方式进行评价.大量的波像差实际检测结果表明,成像集中度和成像能量分布在不同的检测分辨率条件下的稳定性较好,分辨率每相差一倍产生的差异通常小于 10%.中频误差含量不同的两个球面和非球面波像差的实例比较结果表明波像差梯度偏离值可以很好地评价波像差的空间频率分布特征.根据出瞳位置的波像差梯度偏离值分布和像面位置的波像差梯度分布情况,可以方便地指导光学加工和系统装调.该方法可以用于制定波像差指标,进行波前质量控制.

关键词:光学工程;光学检测;波像差检测;波像差梯度

中图分类号:O439 **文献标识码**:A **文章编号**:1004-4213(2015)12-1211002-6

Wavefront Gradient Deviation Evaluation Methods

SONG Shu-mei

(*Changchun Institute of Optics, Fine Mechanics and Physics, Chinese Academy of Sciences, Changchun* 130033, *China*)

Abstract: In order to evaluate wavefront of imaging systems, the wavefront gradient deviation evaluation methods were proposed, which could directly indicate imaging performance. The wavefront gradient deviation is defined as the deviation of image spot and image energy center, and the relative wavefront gradient deviation is the ratio of wavefront gradient deviation to Airy disk radius. The wavefront gradient deviation and relative gradient deviation can be evaluated by image size, image concentration and image energy distribution. Based on dozens of practical wavefront testing results, the evaluations of image concentration and image energy distribution are usually stable enough for different test resolutions. The difference of evaluation results is usually less than 10% for every double or half resolution. An aspherical wavefront and a spherical wavefront with dramatically ripple amount were analyzed to illustrate the relationship of wavefront gradient deviation and wavefront spacial distribution. Relied on the wavefront gradient deviation distribution on exit pupil and wavefront gradient distribution on image plane, it is convenient to operate for optical manufacture and assembling. The wavefront gradient deviation evaluations can be used as the wavefront specifications for quality control.

Key words: Optical engineering; Optical testing; Wavefront testing; Wavefront gradient

OCIS Codes: 350.4600; 120.4800; 220.4840; 120.5050

0 Introduction

Wavefront evaluation[1] is of significant importance to optical design, manufacture and system assembling. The most popular evaluation methods, Peak-to-Valley (PV) and Root Mean Square (RMS), have been recorded in ISO 10110[2-5]. PV and RMS are sensitive to wavefront magnitude, however, they can't represent

Foundation item: The Third Phase of Knowledge Innovation Project of CAS (No. XXX)

First author: SONG Shu-mei (1963—), female, professor, bachelor's degree, mainly focuses on optical testing and manufacturing of large aspheres. Email: smsong@ciomp.ac.cn

Received: Sep. 21, 2015; **Accepted**: Nov. 4, 2015

spacial distribution information of wavefront. In order to represent the spacial distribution information, Power Spectral Density (PSD)[6-9] can be used, which has been playing a very important role in National Ignition Facility (NIF)[10-12] since 1990s. It indicates the cosine-shape components of different spacial frequency composing a wavefront or a slice of the wavefront. PSD is also recorded in ISO, however, ISO only gives the definition of a wavefront slice. The PSD curve could be totally different when the data of several pixels on the marginal wavefront are changed. PSD is not widely used in imaging system. Besides ISO, Peak-to-Valley Robust (PVr)[13], proposed by ZYGO Corp., has been used in MetroPro version 8.3.1, it is a combination of PV and rms but is more stable than PV. Wavefront gradient[14-19] is another evaluation method that can indicate wavefront spatial distribution. On the other hand, it is also an indication of image performance. However, wavefront gradient is reverse proportional to wavefront dimension, it is not convenient to be used as the specification standard for wavefront evaluation.

In order to indicate image performance more precisely for imaging systems, the evaluation methods of wavefront gradient deviation is proposed. On the basis of wavefront gradient deviation, the relative wavefront gradient deviation is proposed so that the wavefront evaluation can be independent on wavefront dimension.

1 Wavefront gradient deviation

1.1 Definition of wavefront gradient deviation

Assuming there is a converging wavefront of Zernike coma at a normalize circular exit pupil, shown in Fig. 1. The wavefront can be described as

$$W=3\cdot x^2\cdot y+3\cdot y^3-2\cdot y \tag{1}$$

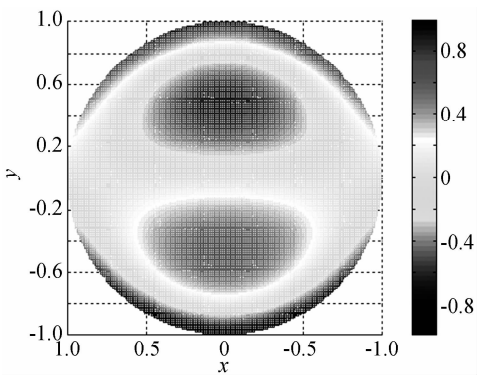

Fig. 1 Wavefront distribution of Zernike coma

According to geometric optical theory, the ray emerging from point (x,y) at the exit pupil is different from the one emerging from a perfect wavefront. The deviation angle is the wavefront gradient, $\partial W/\partial x$ and $\partial W/\partial y$, in x and y direction, respectively. The wavefront gradient distribution on image plane is coincident with the image distribution. But it is different from Point Spread Function (PSF) for it ignores diffraction. When the diameter of exit pupil is $D=100$ mm, the wavefront gradient distribution on image plane is shown in Fig. 2.

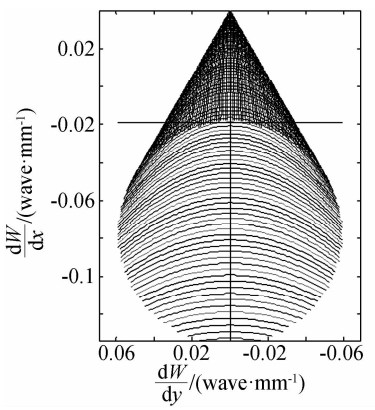

Fig. 2 Wavefront gradient distributions on image plane of Zernike coma

In the case of uniform intensity, the angular center of the image energy locates at the mean value of wavefront gradient $(\overline{\partial W/\partial x},\overline{\partial W/\partial y})$, shown as the cross in Fig. 2.

$$\begin{cases}\overline{\dfrac{\partial W}{\partial x}}=\dfrac{1}{n}\cdot\sum\limits_{i=1}^{n}\dfrac{\partial W}{\partial x_i}\\ \overline{\dfrac{\partial W}{\partial y}}=\dfrac{1}{n}\cdot\sum\limits_{i=1}^{n}\dfrac{\partial W}{\partial y_i}\end{cases} \tag{2}$$

If the intensity is not uniform, the location of image energy center is relative to the weight of intensity m

$$\begin{cases}\overline{\dfrac{\partial W}{\partial x}}=\left[\sum\limits_{i=1}^{n}\left(m_i\cdot\dfrac{\partial W}{\partial x_i}\right)\right]/\sum\limits_{i=1}^{n}m_i\\ \overline{\dfrac{\partial W}{\partial y}}=\left[\sum\limits_{i=1}^{n}\left(m_i\cdot\dfrac{\partial W}{\partial y_i}\right)\right]/\sum\limits_{i=1}^{n}m_i\end{cases} \tag{3}$$

When using image energy center as the evaluation standard, the imaging performance of the wavefront can be evaluated by wavefront gradient deviation, defined as the difference between each image position and the energy center

$$\mathrm{GD}=\sqrt{\left(\frac{\partial W}{\partial x}-\overline{\frac{\partial W}{\partial x}}\right)^2+\left(\frac{\partial W}{\partial y}-\overline{\frac{\partial W}{\partial y}}\right)^2} \tag{4}$$

The corresponding distribution of wavefront gradient deviation on exit pupil is shown in Fig. 3. The coordinates are identical to wavefront distribution in Fig. 1.

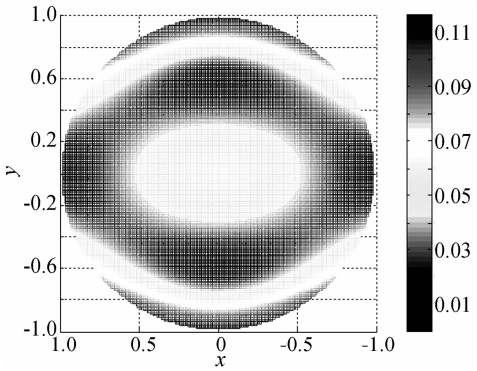

Fig. 3 Wavefront gradient deviation distributions on exit pupil of Zernike coma

1.2 Preprocess for wavefront gradient deviation evaluation

Wavefront gradient deviation is the deviation of wavefront gradient from the mean value. It is not necessary to process wavefront piston and tilt because they are automatically removed when calculating the gradient and the deviation of gradient, respectively.

Power, defined by MetroPro of Zygo Corp., can be sometimes removed before wavefront evaluating when defocus can be introduced. Fig. 4 is the distribution of the 9th Zernike wavefront (the 3rd spherical aberration) and its wavefront gradient distribution on imaging plane for $D = 100$ mm. For tightening image, some defocus is introduced, shown in Fig. 5. Note the scales in Fig. 4 and Fig. 5 are different. The best amount of the introduced defocus depends on the wavefront evaluation method, which will be described in Section 2. Similarly, the approaches

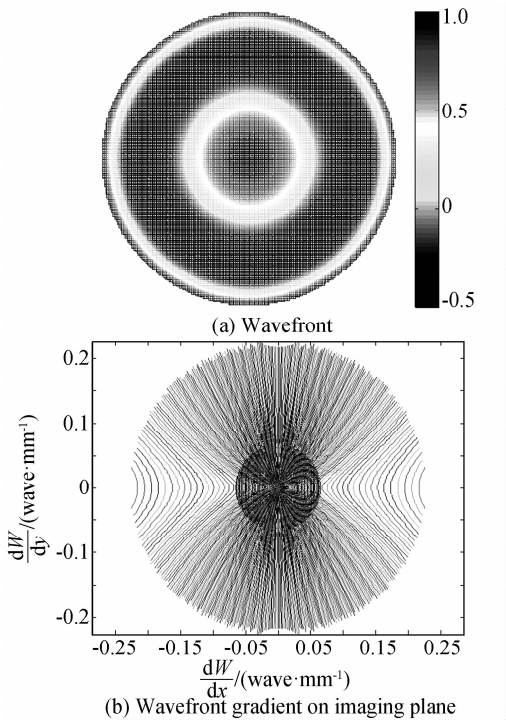

Fig. 4 Distribution of the 9th Zernike wavefront and its wavefront gradient distribution on imaging plane

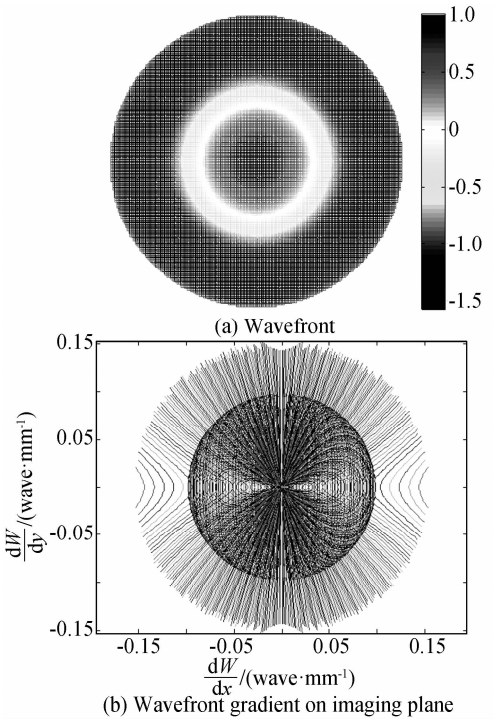

Fig. 5 Distribution of the 9th Zernike wavefront with the best defocus amount introduced and its wavefront gradient distribution on imaging plane

of removing other aberrations are also dependent on evaluation method.

1.3 Evaluations of wavefront gradient deviation

In order to indicate imaging performance, wavefront gradient deviation can be evaluated by the following methods.

1.3.1 *Image size*

Image size is the range of all image points on the image plane. It can be evaluated by the maximum of gradient deviation

$$GD_{max} = \max(GD) \tag{5}$$

All the image points can be included in a circle which is centered at $(\overline{\partial W/\partial x}, \overline{\partial W/\partial y})$ and has the radius of GD_{max}.

1.3.2 *Image concentration*

Image concentration is the denseness of image points. It can be evaluated by the mean value or root mean square of wavefront gradient deviation. In the case of uniform intensity

$$\begin{cases} \overline{GD} = \dfrac{1}{n} \cdot \sum_{i=1}^{n} GD_i \\ RMSGD = \sqrt{\dfrac{1}{n} \cdot \sum_{i=1}^{n} GD_i^2} \end{cases} \tag{6}$$

In the case of nonuniform intensity,

$$\begin{cases} GD = \left[\sum_{i=1}^{n} (m_i \cdot GD_i)\right] / \sum_{i=1}^{n} m_i \\ RMSGD = \sqrt{\left[\sum_{i=1}^{n} (m_i \cdot GD_i^2)\right] / \sum_{i=1}^{n} m_i} \end{cases} \tag{7}$$

1.3.3 *Image energy distribution*

When drawing a circle of its center at ($\overline{\partial W/\partial x}$, $\overline{\partial W/\partial y}$), the image energy distribution can be presented by a curve, of which the abscissa is the circular radius and the ordinate is the percentage of image points included in the circle. The two points (0, 0) and (GD_{max}, 100) are always passed through by the curve. The wavefront gradient distribution on imaging plane in Fig. 2 can be transformed into the image energy distribution curve in Fig. 6. The image radius corresponding to any concerned energy threshold can be found in the curve. For example $GD_{84\%}$ is the radius corresponding to 84% of the image energy.

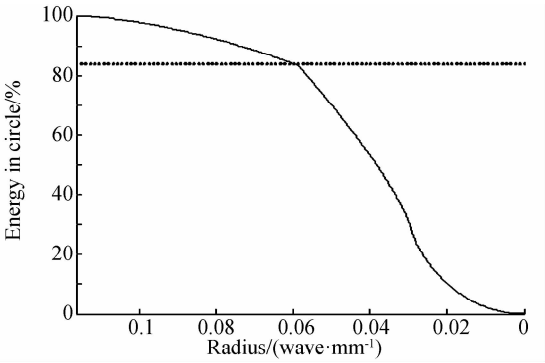

Fig. 6 Image energy distribution curve of Zernike coma

The physical significance of image energy distribution curve is similar to encircled energy curve. But the encircled energy curve is based on diffractive theory. It is the transformation from PSF. The image energy distribution curve could be more precise for the evaluation standard at the energy center. However, the image energy curve would be imprecise, especially when the wavefront is of diffractive quality.

1.4 Disadvantage of wavefront gradient deviation

Wavefront gradient deviation is sensitive to most wavefront distributions. However, it is insensitive to some steep changes such as a step function over the wavefront, shown in Fig. 7. The step function wavefront error usually appears during the manufacture of aspherical components with large asphericity gradient and the assembling of stitching subapertures[20-21]. It doesn't cause much influence on imaging performance and can't be availably evaluated by wavefront gradient deviation evaluations especially by image concentration evaluations. But it can be specified by RMS. The wavefront gradient evaluations can be associated with other specifications such as RMS if it is necessary to avoid step function errors.

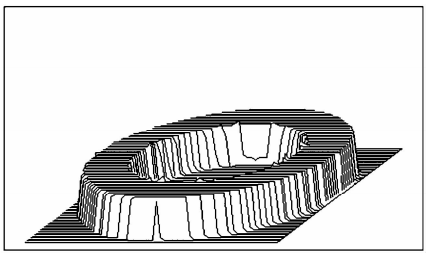

Fig. 7 Step function error over the wavefront

2 Relative wavefront gradient deviation

According to diffractive theory, a perfect uniform converging wavefront forms an Airy disk. The angular radius of central spot is

$$\theta_0 = 1.22\lambda/D \tag{8}$$

where λ is wavelength and D is wavefront diameter. The wavefront gradient deviation is also inverse proportional to wavefront dimension. In order to evaluate wavefront gradient deviation independent on wavefront dimension, the relative gradient deviation is defined as

$$GD_{\theta_0} = GD/\theta_0 \tag{9}$$

No matter the wavefront dimension and focal length, the ratio of image spot to Airy disk will be a constant as long as the wavefront maintains the same distribution and magnitude. Similar to the evaluations of wavefront gradient deviation, the evaluations of relative gradient deviation are defined as

$$\begin{cases} GD_{\max\theta_0} = GD_{\max}/\theta_0 \\ \overline{GD}_{\theta_0} = \overline{GD}/\theta_0 \\ RMSGD_{\theta_0} = RMSGD/\theta_0 \\ GD_{84\%\,\theta_0} = GD_{84\%}/\theta_0 \end{cases} \tag{10}$$

The amount of introduced defocus in Fig. 5 is actually for minimum $RMSGD_{\theta_0}$. The RMS of the wavefront in Fig. 4 and Fig. 5 increases from 0.447λ to 0.697λ, while $RMSGD_{\theta_0}$ decreases from 7.67 to 6.38.

According to Eq. (4) and Eq. (9), relative wavefront gradient deviation is proportional to wavefront magnitude. When the RMS of 4th to 36th Zernike wavefront is normalized to 1λ with no power removed, the distribution of relative wavefront gradient deviation evaluations is shown in Fig. 8. The wavefront appears in power/ spherical aberration, astigmatism and coma/ tilt in turn periodically. The evaluations of relative gradient deviation periodically increase because of the higher spacial frequency of wavefront distribution.

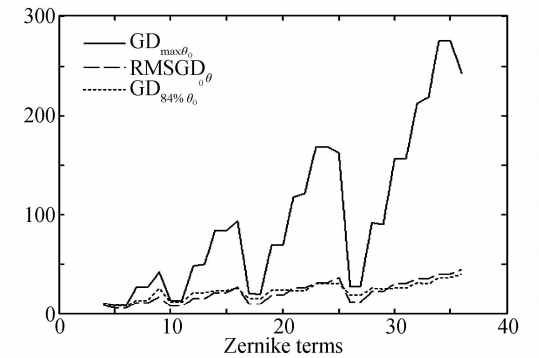

Fig. 8 Distribution of relative wavefront gradient deviation evaluations of 4th to 36th Zernike wavefront

3 Experiments and analysis

Fig. 9 and Fig. 10 are the distributions of a spherical wavefront and an aspherical wavefront, respectively. The spherical wavefront is much smoother with less manufacture footprints than the aspherical wavefront. When scaling wavefront magnitudes to the same RMS results, the image energy distribution curve of the spherical wavefront is steeper and the wavefront gradient deviation evaluations are smaller, as shown in Table 1. This represents fewer ripples (mid-spatial-frequency errors)[22] in the wavefront.

When using a test instrument such as a digital interferometer with higher resolution, the wavefront can be detected in more details. The wavefront gradient deviation evaluations will give different results. If the wavefront is smooth enough so that the influence of the instrument resolution can be ignored, the evaluations of relative gradient deviation will be independent on test resolution. They depend only on the wavefront magnitude and spacial distribution. Based on the statistics of dozens of wavefront testing results of optical components and systems, for the smooth wavefront like flat and spherical wavefront in Fig. 9, the differences of image concentration evaluations and image energy distribution evaluations, such as RMSGD$_{\theta_0}$ and GD$_{84\%\theta_0}$, are usually less than 2% for every double or half resolution differences. The differences are usually less than 10% for the wavefront with lots of ripples like aspherical wavefront in Fig. 10. They are stable enough to be used as the wavefront specifications. However, the stability of GD$_{max\theta_0}$ is not

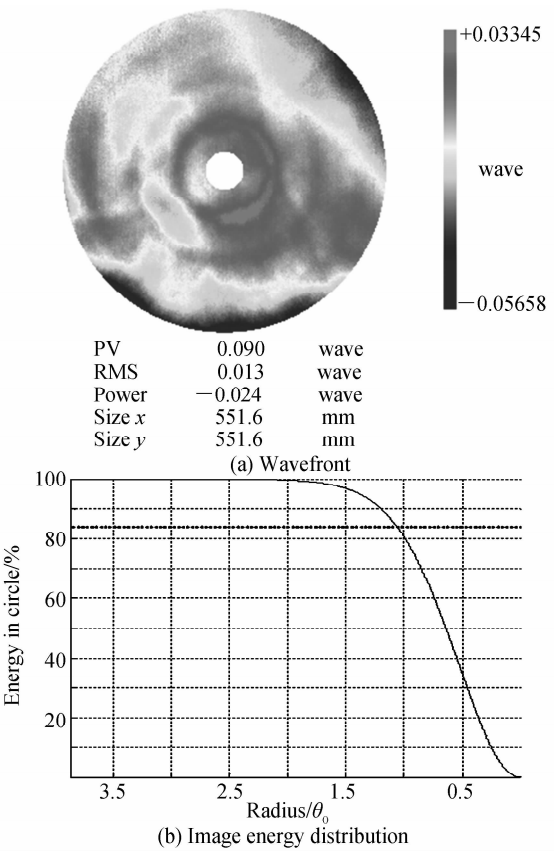

Fig. 9 Wavefront distribution and image energy distribution of wavefront No. 1

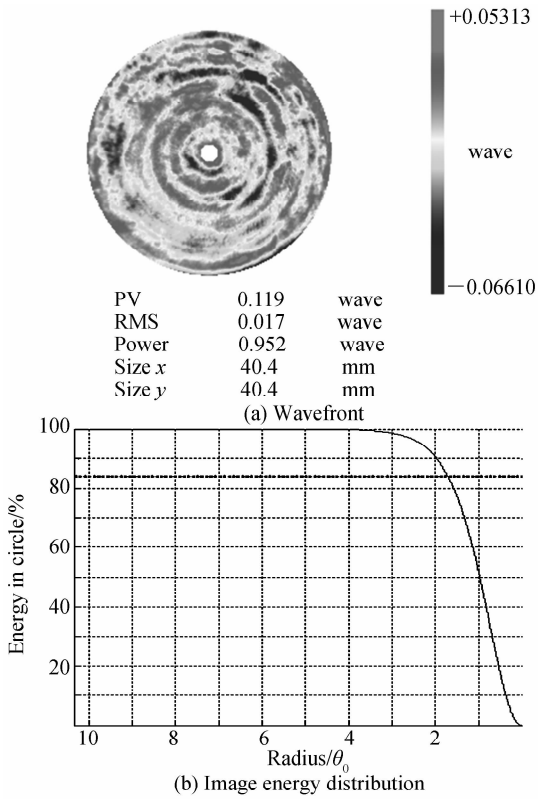

Fig. 10 Wavefront distribution and image energy distribution of wavefront No. 2

Table 1 Evaluations of No. 1 and No. 2 wavefront

Item	No. 1	No. 2
PV/λ	0.090	0.119
RMS/λ	0.013	0.017
GD$_{max\theta_0}$	3.87	10.3
RMS(GD$_{\theta_0}$)	0.790	1.27
GD$_{84\%\theta_0}$	1.06	1.70
GD$_{max\theta_0}$ / RMS	298	605
RMS(GD$_{\theta_0}$)/RMS	60.8	74.7
GD$_{84\%\theta_0}$ / RMS	81.5	100

satisfying. The evaluation differences caused by test resolution can be more than 50%. It is recommended to use image concentration evaluations and image energy distribution evaluations for wavefront quality control.

Because of the identical coordinates to wavefront distribution, the wavefront gradient deviation distribution on exit pupil gives clear instruction to optical manufacture. As shown in Fig. 3, the color bar indicates different process to be carried on. If the red zones on the optical surface are polished properly, the image distribution will be tightened towards the image energy center so as to improve the gradient deviation evaluations. Relied on the wavefront gradient distribution on imaging plane without wavefront reconstruction[23-24], the Computer-Aided Alignment (CAA) technology can be applied on system assembling, especially for the period when the wavefront is beyond the measurement range of interferometric test instruments. Several image distributions of different defocus amounts will be necessary for every alignment in order to interpret the image distribution correctly[25]. The specifications of wavefront gradient deviation especially relative gradient deviation are convenient for the opticians to operate.

4 Conclusion

The wavefront gradient deviation is closely related to the performance of imaging systems. The relative wavefront gradient deviation is independent on the wavefront dimension. The image concentration evaluations and image energy distribution evaluations are usually stable for different test resolutions. The gradient deviation distribution on exit pupil and the wavefront gradient distribution on imaging plane give clear instruction for optical manufacture and system assembling. It is suitable to use gradient deviation evaluations as the wavefront specifications during the process and in the final inspection.

Acknowledgements

Special thanks to Prof. XIE Jing-jiang, Dr. XUAN Bin and Large Lightweighted Mirror Lab in Changchun Institute of Optics, Fine Mechanics and Physics for the technique and funding support.

Reference

[1] MALACARA D. Optical shop testing[M]. New York, Chichester, Brisbane, Toronto, Singapore: Wiley-Interscience, 1992: Chap. 13.

[2] SELBERG L A, TRUAX B E. ISO figure specification (ISO 10110-5) and digital interferometry[C]. Proceedings SPIE, 1992, **1776**: 86-93.

[3] ENGLISH R E JR, AIKENS D M, WHISTLER W T, *et al*. Implementation of ISO 10110 optics drawing standards for the National Ignition Facility[C]. SPIE, 1995, **2536**: 51-56.

[4] WANG D Y, ENGLISH R E JR, AIKENS D M. Implementation of ISO 10110 optics drawing standards for the National Ignition Facility[C]. SPIE, 1999, **3782**: 502-508.

[5] KIONTKE S R, AIKENS D M, YOUNGWORTH R N. Description and tolerancing of freeform surfaces in standards [C]. International Optical Design Conference (Optical Society of America, 2014): ITh3A. 2.

[6] LAWSON J K, WOLFE C R, MANES K R, *et al*. Specification of optical components using power spectral density function[C]. SPIE, 1995, **2536**: 38-50.

[7] YOUNGWORTH R N, GALLAGHER B B, STAMPER B L. An overview of power spectral density (PSD) calculations[C]. SPIE, 2005, **5869**: 58690U.

[8] XU Fang, WEI Quan-zhong, WU Fan. Evaluating intermediate frequency error property of optical profile with density function of power spectrum [J]. *Opto-Electronic Engineering*, 1999, **26**(Sup): 139-143.

[9] YANG Fei, AN Qi-chang, ZHANG Jing-xu. Mirror surface figure evaluation based on power spectral density[J]. *Chinese Optics*, 2014, **7**(1), 156-162.

[10] AIKENS D M, WOLFE C R, LAWSON J K. The use of power spectral density (PSD) functions in specifying optics for the National Ignition Facility[C]. SPIE, 1995, **2576**: 281-292.

[11] AIKENS D M. The origin and evolution of the optics specifications for the national ignition facility[C]. SPIE, 1995, **2536**: 2-12.

[12] WOLFE C R, LAWSON J K. The measurement and analysis of wavefront structure from large aperture ICF optics[C]. SPIE, 1995, **2633**: 361-385.

[13] EVANS C J. PVr - a robust amplitude parameter for optical surface specification[J]. *Optical Engineering*, 2009, **48**(4): 043605.

[14] LAWSON J K, AUERBACH J M, ENGLISH R E JR, *et al*. NIF optical specifications - the importance of RMS gradient [C]. SPIE, 1999, **3492**: 336-343.

[15] LAWSON J K, AIKENS D M, ENGLISH R E JR, *et al*. Surface figure and roughness tolerances for NIF optics and the interpretation of the gradient, P-V wavefront and RMS specifications[C]. SPIE, 1999, **3782**: 510-517.

[16] PUGH W N L, LOBB D R, WALKER D D, *et al*. Pupil-imaging wavefront gradient sensor[C]. SPIE, 1995, **2534**: 312-317.

[17] BARBERO S, RUBINSTEIN J, THIBOS L N. Wavefront sensing and reconstruction from gradient and Laplacian data measured with a Hartmann-Shack sensor[J]. *Optics Letters*, 2009, **31**(12): 1845-1847.

[18] XUAN Bin, LI Jun-feng, Wang Peng, *et al*. Supplemental optical specifications for imaging systems: parameters of phase gradient[J]. *Optical Engineering*, 2009, **48**(12): 123401.

[19] YANG Fei, LIU Jun-guo, AN Qi-chuang, *et al*. Method of evaluation of a mirror surface figure based on frequency and its application for the giant steerable science mirror of the thirty meter telescope[J]. *Chinese Optics Letters*, 2015, **13**(4): 041201.

[20] LIN Xu-dong, WANG Jian-li, LIU Xin-yue, *et al*. Co-phase experiment of active optics for segmented-mirrors[J]. *Optics Precision Engineering*, 2010, **18**(7), 1520-1528.

[21] LIN Xu-dong, CHEN Tao, WANG Jian-li, *et al*. Co-focus experiment of segmented-mirrors for active optics[J]. *Optics Precision Engineering*, 2010, **18**(3), 563-569.

[22] WOLFE C R, DOWNIE J D, LAWSON J K. Measuring the spatial frequency transfer function of phase-measuring interferometers for laser optics[C]. SPIE, 1996, **2870**: 553-557.

[23] XU Hong-yuan, XIANHao, ZHANG Yu-dong. Algorithm and experiment of whole-aperture wavefront reconstruction from annular subaperture Hartmann-Shack gradient data[J]. *Optics Express*, 2010, **18**(13): 13431-13443.

[24] MOCHI I, GOLDBERG K A. Modal wavefront reconstruction from its gradient[J]. *Applied Optics*, 2015, **54**(12): 3780-3785.

[25] MALACARA D. Optical shop testing[M]. New York, Chichester, Brisbane, Toronto, Singapore: Wiley-Interscience, 1992: Chap. 8, 10.